

Observability and Identifiability Analyses of Process Models for Agricultural Anaerobic Digestion Plants

Simon Hellmann¹, Arne-Jens Hempel², Stefan Streif³, Sören Weinrich^{4,1}

¹ DBFZ Deutsches Biomasseforschungszentrum gGmbH, Leipzig, Germany,
{simon.hellmann, soeren.weinrich}@dbfz.de

² Saxon University of Cooperative Education, Glauchau, Germany,
arne-jens.hempel@ba-sachsen.de

³ Chemnitz University of Technology, Chemnitz, Germany,
stefan.streif@etit.tu-chemnitz.de

⁴ Münster University of Applied Sciences, Faculty of Energy · Building Services ·
Environmental Engineering, Münster, Germany, weinrich@fh-muenster.de

This is the extended version of an accepted paper submitted to the 24th International Conference on Process Control on April 4, 2023. The extended version is available under a CC BY-NC-ND 4.0 license.

Abstract

Dynamic operation of anaerobic digestion plants requires advanced process monitoring and control. Different simplifications of the Anaerobic Digestion Model No. 1 (ADM1) have been proposed recently, which appear promising for model-based process automation and state estimation. As a fundamental requirement, observability and identifiability of these models are analyzed in this work, which was pursued through algebraic and geometric analysis. Manual algebraic assessment was successful for small models such as the ADM1-R4 and simplified versions of the ADM1-R3, which were derived in this context. However, for larger model classes the algebraic approach showed to be insufficient. By contrast, the geometric approach, implemented in the STRIKE_GOLDD toolbox, allowed to show observability for more complex models (including ADM1-R4 and ADM1-R3), employing two independent algorithms. The present study lays the groundwork for state observer design, parameter estimation and advanced control resting upon ADM1-based models.

Key words: ADM1, model simplification, Biogas technology, parameter estimation, STRIKE_GOLDD

1 Introduction

Anaerobic digestion (AD) allows to convert numerous organic feedstocks into biogas, which can either be upgraded and injected into the natural gas grid or combusted to produce renewable electricity and heat.

The AD process naturally shows strongly nonlinear behavior and is sensitive to process inhibition [1]. Moreover, the process is prone to instability, especially during dynamic feeding [2]. To avoid instable process behavior, monitoring and control schemes are required.

Many investigations focus on automated operation of domestic or industrial wastewater treatment plants [3–6]. Additionally, advanced control for efficient and demand-oriented biogas production of agricultural AD plants are frequently examined [2, 7, 8].

A bottleneck in full-scale application of AD is the lack of online measurements, especially regarding reliable stability indicators, such as volatile fatty acids (VFA) and alkalinity [9]. A remedy to overcome this shortage is to apply soft sensors (or state observers), which use readily available external measurements and a mathematical model of the process to estimate internal, non-measurable process states [10].

A prominent process model was presented by Bernard et al. [11], which has successfully been used in multiple monitoring and control applications [3, 4, 12].

However, nonlinear aspects of the AD process are described in more detail within the established Anaerobic Digestion Model No. 1 (ADM1) [13]. While the model proposed by Bernard et al. only includes pH inhibition, the ADM1 covers process inhibition through pH, nitrogen limitation and ammonia. Still, successful applications of the ADM1 in full-scale monitoring and control applications have not yet been reported, mostly because of its complexity and vast number of parameters [14].

Yet, in an agricultural setting, which is an important application of AD, both the original ADM1 and the model by Bernard et al. cannot directly be used due to their underlying reference unit (chemical oxygen demand, COD) [15]. Thus, Weinrich and Nelles have recently proposed mass-based simplifications of the ADM1 [15, 16]. These models represent a suitable alternative for application in monitoring and control of agricultural AD plants [7]. Individual model variations differ significantly in their number of differential equations, state variables and required parameters (Fig. 1). Simplified models (such as the ADM1-R4) combine nutrient degradation and biogas formation based on first-order sum reactions, whereas more detailed models (such as the ADM1-R3) depict specific degradation pathways and ammonia or pH inhibition during acetoclastic methanogenesis.

Observability is a model property which indicates whether internal states can be inferred based on input-output measurements [17]. Likewise, identifiability implies that model parameters can be calibrated based on input-output measurements. Assessing observability and identifiability is therefore a fundamental requirement before implementing state and parameter estimation.

Numerous approaches for assessing observability and identifiability have been proposed [18–20]. However, especially for complex models they are seldom analyzed a priori because of the computational complexity of the symbolic calculations involved [20].

This contribution analyzes observability and identifiability of different ADM1 simplifications proposed by Weinrich and Nelles [15]. For this purpose, two different approaches are pursued: the differential algebraic and differential geometric approach.¹ Typical measurements at full-scale AD plants are assumed to be available to ensure feasibility of future process control schemes based on these analyses.

2 Methods

In this work, we consider systems of ordinary differential equations of the form:

$$M : \begin{cases} \dot{x} &= f(x(t), u(t), \theta) \\ y &= h(x(t), \theta) \\ x(t_0) &= x_0 \end{cases} \quad (1)$$

with state variables $x \in \mathbb{R}^n$, initial state x_0 , manipulated variables $u \in \mathbb{R}^p$, measurement variables $y \in \mathbb{R}^q$, and model parameters $\theta \in \mathbb{R}^m$. Generally, model parameters (such as microbial growth or decay rates) can be time-variant. However, they vary at a slow rate of change and their dynamics do not follow a defined differential equation. Therefore, their implicit time dependence is suppressed in the notation.

2.1 Modelling of the Anaerobic Digestion Process

Based on available model simplifications in Fig. 1, observability and identifiability were assessed for the ADM1-R4, ADM1-R3 and ADM1-R2 [15]. Mass concentration of ash was integrated to compute volatile solids (VS) measurements.

¹The two approaches are simply referred to as algebraic and geometric in the following.

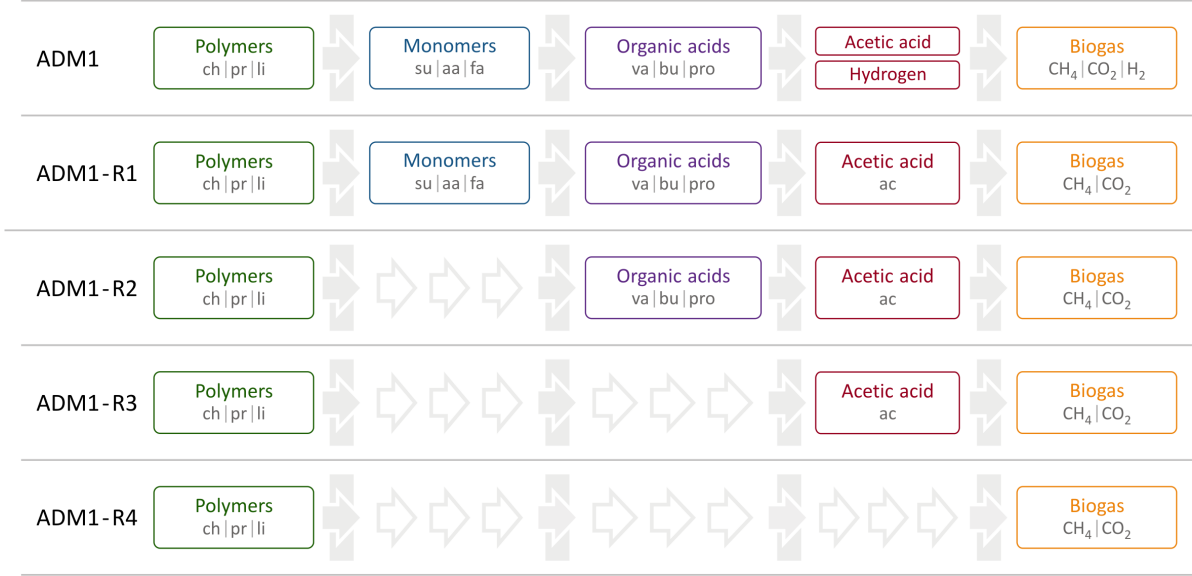


Figure 1: Characteristics of different ADM1 simplifications [15].

2.1.1 Model Simplification

Both ADM1-R4 and ADM1-R3 were further simplified throughout the investigation. For this purpose, individual model components were isolated and omitted or incorporated systematically to assess their influence on observability. Fig. 2 illustrates the full ADM1-R4 and its model parts qualitatively. These model parts are decay of microbial biomass and its stoichiometric feedback as macro nutrients (part A, in green), and gas solubility of methane and carbon dioxide (part B, in orange).

The ADM1-R3 allows to isolate more model parts as shown in Fig. 3. Part A and B were left identical as for the ADM1-R4 (in green and orange, respectively). Part C (in purple) describes inhibition through nitrogen limitation. Part D (in blue) covers inhibition through pH and ammonia, as well as dissociation of ammonium/ammonia. Lastly, part E (in red) contains the computation of pH, which includes the charge balance of available anions and cations.

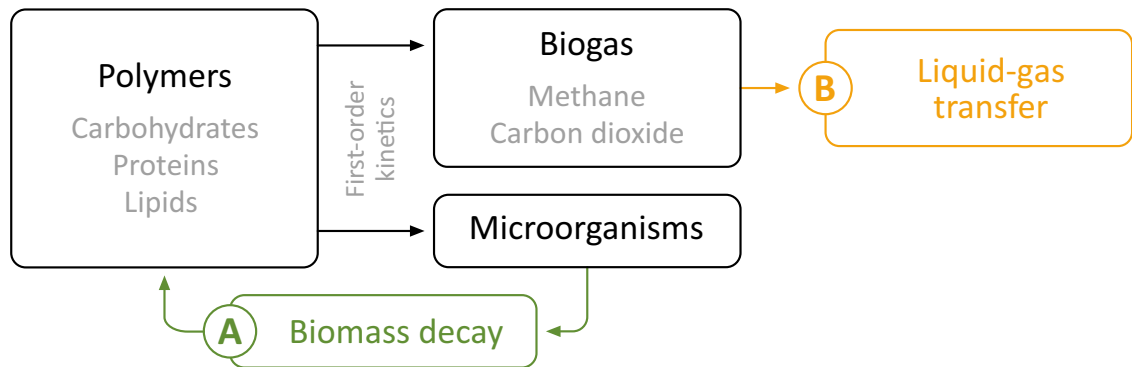


Figure 2: Model components of the ADM1-R4.

The core elements of the models ADM1-R4 and ADM1-R3 without any additional model parts are denoted as BMR4 and BMR3 (base model, BM). Augmenting them with additional model parts results in e.g. BMR4+A. The same notation applies for individual ADM1-R3 model variations. The investigated models are summarized in Tab. 2. A full set of the corresponding model equations is given in the appendix.

2.1.2 Data Availability

For observability and identifiability analyses, measurement signals in Tab. 1 were considered. Online measurements were generally restricted to pH and gas composition, expressed as partial pressures of methane and carbon dioxide [21]. For detailed assessment of observability using the algebraic approach, acetic acid was also considered as available online. For lab and pilot-scale settings, this is a reasonable assumption [22]. Generally, however, online measurements of acetic acid were not considered, which represents the more realistic scenario in a full-scale agricultural setting [21].

Offline measurements of total solids (TS), volatile solids (VS) and inorganic nitrogen (IN) were assumed to be slowly time-variant in between samples [23]. To obtain time-continuous signals, sample-and-hold behavior was supposed.

2.2 Observability Analyses

Definition. A state variable $x_i(t)$ is observable if its initial state $x_i(0)$ can be reconstructed from measurements of inputs $u(\tau)$ and outputs $y(\tau)$ over a finite time $\tau \in [0, t]$. A system M is fully observable if all of its n states are observable. If at least one state is not observable, the system is not fully observable [24].

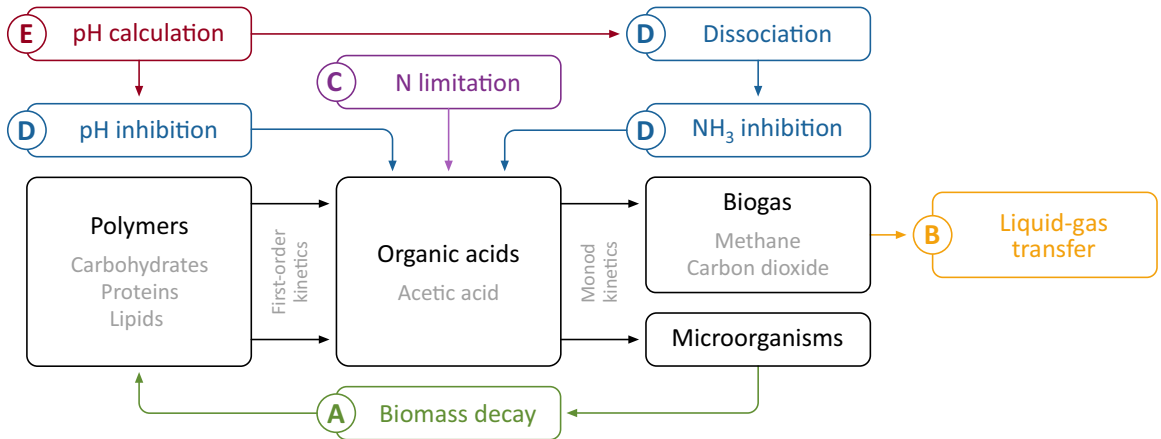


Figure 3: Model components of the ADM1-R3.

In this work, two pathways to assess observability were pursued: the algebraic and the geometric approach. In the former, a system of equations of output variables and their time derivatives is established and solved for individual model states. The latter assesses the observability rank condition, which relies on an observability matrix.

2.2.1 Algebraic Approach

In the algebraic approach, a system of equations of output variables y and their time derivatives $y, \dot{y}, \ddot{y}, \dots$ is established and solved for the state variables $x_i, i \in 1, \dots, n$. The system of equations can be summarized as

$$\mathcal{Y} = \mathcal{Y}(x, u, \theta), \text{ where } \mathcal{Y} = (y, \dot{y}, \ddot{y}, \dots)^T. \quad (2)$$

Time derivatives of the outputs are obtained by iteratively computing the Lie derivatives with respect to f . We assumed constant input signals during individual feeding events ($\dot{u} = 0$) and constant parameters ($\dot{\theta} = 0$), resulting in:

$$y = h(x, \theta) \quad (3)$$

$$\dot{y} = L_f h(x, \theta) = \frac{\partial h(x, \theta)}{\partial x} f(x, u, \theta), \quad (4)$$

$$\ddot{y} = L_f^2 h(x, \theta) = \frac{\partial L_f h(x, \theta)}{\partial x} f(x, u, \theta), \quad (5)$$

$$\vdots$$

$$y^{(k)} = L_f^{(k)} h(x, \theta) = \frac{\partial L_f^{(k-1)} h(x, \theta)}{\partial x} f(x, u, \theta). \quad (6)$$

Observability is given if the system of equations (2) can be solved algebraically for all states $x_i, i = 1 \dots n$ and has at least one solution [17]. This requires n equations, which can either be obtained by incorporating all of the q entries of each vector y, \dot{y} etc.; or by building higher-order time derivatives $y^{(k)}$ and incorporating their elements. If the system of equations can be solved uniquely, global observability is shown. Multiple solutions indicate local observability [17].

Table 1: Measurement signals considered for individual model classes

Model class	Online	Offline ^a
ADM1-R4	gas composition (CH ₄ , CO ₂)	TS, VS, IN
ADM1-R3 ^b	gas composition (CH ₄ , CO ₂), pH	TS, VS, IN

^aTotal solids (TS), volatile solids (VS) and inorganic nitrogen (IN)

^bDuring algebraic observability analyses acetic acid was also considered as an optional online measurement.

Implementation The algebraic approach was implemented in Mathematica (version 13.0, Wolfram Research, Inc.). Equations which could be solved for state variables manually were excluded from the system of equations to minimize computational demand. Complexity of the system of equations was further reduced by seeking to incorporate terms with minimal orders of time derivatives first. This is because generally complexity of symbolic derivatives $y^{(k)}$ increases rapidly with the order of derivatives k [20]. Selection of terms among the q elements of $y^{(k)}$ followed a heuristic procedure.

Since the algebraic approach turned out to be inconclusive for the ADM1-R3, the models ADM1-R4 and ADM1-R3 were systematically simplified (see Sec. 2.1). The maximum allowable model complexity for the algebraic approach was determined by systematically adding model components, starting from the base models (BMR4 and BMR3), and terminating when the system of equations could no longer be solved.

In the algebraic approach, all parameters and influent concentrations were assumed to be known and time-invariant. Moreover, for the ADM1-R3 model classes, measurements of acetic acid were assumed to be available online in order to achieve conclusive statements on observability, see Sec. 3.1.

2.2.2 Geometric Approach

In the differential geometric approach observability is investigated by computing the rank of an observability matrix. Two different algorithms were considered in this context, which differ in the way the observability matrix is built: Full Input-State-Parameter Observability (FISPO) and Observability Rank Condition with Direct Feedthrough (ORC-DF). Both algorithms rely on Lie derivatives of the output. For better understanding, computation of the observability matrix is explained by means of the FISPO algorithm. In a second step, disparities with respect to the ORC-DF algorithm are illustrated.

In FISPO, the observability matrix $\mathcal{O}(x)$ is built by taking the Lie derivatives of the output symbolically and computing their partial derivatives with respect to the states x :

$$\mathcal{O}(x) = \begin{pmatrix} \frac{\partial h(x)}{\partial x} \\ \frac{\partial}{\partial x} (L_f h(x)) \\ \vdots \\ \frac{\partial}{\partial x} (L_f^{n-1} h(x)) \end{pmatrix}. \quad (7)$$

A model is locally observable in a neighborhood $N(x_0)$ of a point x_0 if it holds that [18]

$$\text{rank}(\mathcal{O}(x_0)) = n. \quad (8)$$

The ORC-DF algorithm pursues a different approach in computing the observability matrix and is only applicable for input-affine systems [19], which can be described as:

$$\dot{x} = f(x) + \sum_{j=1}^p g_j(x)u_j, \quad (9)$$

$$y = h_0(x) + \sum_{j=1}^p h_j(x)u_j. \quad (10)$$

$f, g_j \in \mathbb{R}^n$ and $h_0, h_j \in \mathbb{R}^p$ are vectorial functions, which describe the output y uniquely. They are aggregated in a column vector Ω . The observability matrix in ORC-DF is built repeatedly using symbolic computation. Initially, it is computed as partial derivatives of Ω with respect to the states x . If the observability rank condition can be satisfied, the system is locally observable. If not, the vector Ω is extended by the Lie derivatives of the previous version of Ω with respect to f and g_j . This procedure continues until the rank condition is satisfied or a maximum number of iterations is reached. Details can be found in [19].

Implementation Both geometric approaches were implemented in the Matlab toolbox STRIKE_GOLDD 4.0 [25]. The toolbox allows to assess local observability (and structural local identifiability) with the FISPO and ORC-DF algorithms.

To ensure that statements on observability of the models are independent from the numeric value of the initial state x_0 , no previously known initial states x_0 were assumed for both procedures. This results in symbolic computations of $\mathcal{O}(x)$ and its rank.

In the geometric approach, full model classes ADM1-R4 and ADM1-R3 as well as all submodels were analyzed. Inlet concentrations were assumed to be known and time-invariant.

Computations of both algebraic and geometric approaches were conducted on a standard personal computer.²

2.3 Identifiability Analyses

Definition. A model parameter $\theta_i, i = 1, \dots, m$ is *structurally identifiable (s.i.)* if for almost all true parameter values θ^* the parameter estimate $\hat{\theta}$ can be determined from input-output behavior of the model M [26]:

$$M(x(t), u(t), \hat{\theta}) = M(x(t), u(t), \theta^*) \quad (11a)$$

$$\Rightarrow \hat{\theta} = \theta^*. \quad (11b)$$

²Intel Core i5 processor (1.7 GHz), 32 GB RAM and Windows 10 operating system.

If all model parameters θ_i are s.i., the model is s.i.. A parameter θ_i is locally structurally identifiable (l.s.i.) if (11) holds in a neighborhood $\mathcal{N}(\theta^)$. A full model is l.s.i. if all its parameters θ_i are l.s.i.. If at least one of them is not, the model is not l.s.i..*

Identifiability was analyzed as part of the differential geometric approach and considered as augmented observability [18, 19]. For this purpose, the state vector is augmented by the model parameters, for which trivial dynamics are assumed:

$$\dot{\tilde{x}} = \begin{pmatrix} \dot{x} \\ \dot{\theta} \end{pmatrix} = \begin{pmatrix} f(x, u, \theta) \\ 0 \end{pmatrix}. \quad (12)$$

Consequently, for FISPO, computation of the extended observability matrix is augmented to:

$$\mathcal{O}(\tilde{x}) = \begin{pmatrix} \frac{\partial h(\tilde{x})}{\partial \tilde{x}} \\ \frac{\partial}{\partial \tilde{x}} (L_f h(\tilde{x})) \\ \vdots \\ \frac{\partial}{\partial \tilde{x}} (L_f^{n+m-1} h(\tilde{x})) \end{pmatrix}. \quad (13)$$

The system is considered observable and identifiable if the rank conditions satisfies [18]

$$\text{rank}(\mathcal{O}(\tilde{x}_0)) = n + m. \quad (14)$$

For ORC-DF the state differential equations (9) are augmented by a zero vector of dimension $m \times 1$, accounting for the trivial dynamics of the parameters. The output equations remain unchanged.

For the ADM1-R4, the rate constants of hydrolysis and decay were assumed as time-variant and analyzed for identifiability. For the ADM1-R3, the following parameters were investigated: maximum growth rate and half-saturation constant of acetoclastic methanogens as well as the inhibition constant for non-competitive ammonia inhibition.

3 Results and Discussion

This section presents the results of both the algebraic and geometric approach. Results of the full model variants are discussed first, followed by the simplified submodels.

3.1 Algebraic Approach

The full ADM1-R4 (BMR4+AB) could be shown to be globally observable. Tab. 2 summarizes the required measurements, time derivatives and computing times for all succesful runs of

Table 2: Measurements and their time derivatives required for algebraic observability of model simplifications

			Nominal measurements ^{a,b}						1 st derivative				2 nd derivative				3 rd deriv. ^e	
Model name	n^c	$t[s]^d$	CH ₄	CO ₂	IN	TS	VS	Ac	CH ₄	CO ₂	IN	TS	CH ₄	CO ₂	IN	TS	CH ₄	CO ₂
BMR4	9	5	x	x	x	x	x		x	x			x	x				
BMR4+A	9	3	x	x	x	x	x		x	x			x	x				
BMR4+B	11	6	x	x	x	x	x		x	x			x	x			x	x
BMR4+AB	11	8	x	x	x	x	x		x	x			x	x			x	x
BMR3 ^f	11	541	x	x	x	x	x	x	x	x	x	x	x					
BMR3+A ^f	11	291	x	x	x	x	x	x	x		x	x	x			x		
BMR3+AC ^f	11	1065	x	x	x	x	x	x	x		x	x	x			x		
BMR3+BC ^f	13	5192	x	x	x	x	x	x	x	x	x	x	x	x		x		
BMR3+ABC ^f	13	10225	x	x	x	x	x	x	x	x		x	x	x			x	x

^aCH₄, CO₂ - partial pressures of methane and carbon dioxide; IN - inorganic nitrogen; TS, VS - total and volatile solids; Ac - acetic acid ^bCH₄ and CO₂ were assumed as online measurements, as well as Ac for ADM1-R3

variants. IN, TS and VS were assumed as offline measurements. ^cNumber of states ^dComputation time

^ederivative ^fOnly local observability could be shown because two solutions to the equation systems were found.

the algebraic approach. Color codes of the submodels are consistent with Fig. 2 and 3. Note that alternative combinations to form the equation systems are possible and result in slightly different computing times. This applies for all successful runs of the algebraic approach. For the ADM1-R4, the underlying system of equations involves online measurements of the gas composition (CH₄ and CO₂). Furthermore, to guarantee observability, measurements of IN, TS and VS need to be available. This follows directly from the model equations: all three states only appear in their corresponding differential equation. Therefore, if they were not available as measurements, they could not be observable because they would not be introduced into the system of equations via other measurements, regardless of the degree of time derivatives.

Model simplifications were applied to the ADM1-R4, resulting in the submodels BMR4, BMR4+A and BMR4+B. This was done to explore the effect of individual model parts on the complexity of the equation system, indicated by the computing time required to solve the system of equations. Neglecting model part B reduced the computing time the most (BMR4+A). Only neglecting model part A (BMR4+B) also reduced computing time, albeit not as much. However, neglecting both model parts A and B (BMR4) resulted in slightly longer computing times than for BMR4+A. This is reasonable because simplifying the stoichiometric degradation pathway for biomass decay (model part A) in fact results in more complex terms for the time derivatives of the gas partial pressures if gas solubility (model part B) is neglected as well.

For the full ADM1-R3 (equivalent to BMR3+ABCDE), the solver of Mathematica failed to deliver conclusive statements on observability, likely due to the complexity of the resulting terms in the system of equations. Neither a set of solutions nor an empty set could be returned. Instead, the kernel systematically died in the process of solving the equation systems. Hence, with the algebraic approach, observability of the full ADM1-R3 could not be determined.

Therefore, model complexity of the ADM1-R3 was reduced by isolating and omitting individual model parts (see Sec. 2.1).

Up to this point, measurements of CH_4 , CO_2 , IN, TS and VS were assumed. Additionally, for all ADM1-R3 submodels online measurements of acetic acid had to be taken into account to show local observability, see Tab. 2. The obtained results are therefore strictly valid only for lab- and pilot-scale settings [22].

With given nominal measurements of VS, it was preferred to include time derivatives of TS over VS because both terms added the same information to the system of equations, but TS delivered less complex terms.

BMR3+ABC is the most complex model variant whose resulting system of equations could still be solved with the algebraic approach, see Tab. 2. Two solutions of the systems of equations were obtained, indicating local observability.

For both BMR3+AC and BMR3+BC, local observability could be shown because two solutions each were obtained. Neglecting model part B reduced the computing time more than neglecting model part A, which is in line with the ADM1-R4 submodels.

When further reducing BMR3+AC by model part C (BMR3+A), the shortest computing times of all ADM1-R3 submodels was achieved. However, omitting all model parts (BMR3) resulted in increased computing time compared with BMR3+A. This is consistent with the findings from the ADM1-R4 submodels.

Higher-order variants than BMR3+ABC result in an increased number of states because computation of pH needs to be considered as well as inhibition through pH and ammonia. This leads to symbolic systems of equations too complex to be solved in the presented framework.

When restricting measurements to gas composition, IN, TS and VS (no measurement of acetic acid), none of the ADM1-R3 submodels could be shown to be observable with the algebraic approach because complexity of the systems of equations increased significantly. This is comprehensible since in this case the state variable of acetic acid needs to be incorporated through higher-order time derivatives of the other measurement equations.

3.2 Geometric Approach

Based on the implementation in the STRIKE_GOLDD toolbox, the geometric approach proved to be successful in showing both local observability and structural local identifiability of the full models ADM1-R4 and ADM1-R3 and all of their submodels. Moreover, this was achieved in (i) shorter computing times, (ii) without assuming acetic acid as an online measurement, and

Table 3: Model properties and computing times of FISPO and ORC-DF algorithms for ADM1-R4, BMR3+ABC and ADM1-R3.

Model class	number of		computing time in s	
	states	parameters	FISPO	ORC-DF
ADM1-R4	11	4	3	7
BMR3+ABC	13	7	12	5
ADM1-R3	17	7	11959	811

(iii) by employing two independent algorithms (FISPO and ORC-DF). Tab. 3 summarizes the computing times for the full models ADM1-R4 and ADM1-R3 as well as for BMR3-ABC, being the most complex model that could successfully shown to be observable with the algebraic approach, cf. Tab. 2. As noted by [27], computational efficiency of FISPO and ORC-DF can differ vastly depending on the model structure, which is especially apparent for the full ADM1-R3.

Furthermore, computational effort decreased significantly when neglecting model parts of the full ADM1-R3: computing times of the submodel BMR3-ABC reduced to 12 and 5 s for FISPO and ORC-DF, compared with about 12,000 and 800 s for the full ADM1-R3, respectively.

Computation times of the geometric approach were generally shorter than for the algebraic one. This is reasonable because in the former only the existence of a solution to the systems of equations is assessed (through the observability rank condition), whereas the equation systems have to be solved explicitly in the latter.

Higher-order model classes such as the ADM1-R2 are of similar structure as the ADM1-R3, but involve significantly more time-variant parameters and contain a more detailed acid spectrum (acetic to valeric acid instead of only acetic acid) [15], and thus more states. In an agricultural setting, these acid measurements are not available online. Even when assuming them to be available online, both algorithms of the geometric approach failed to evaluate the respective observability rank condition, and thus did not allow to draw conclusive statements. This is likely due to the aggravated complexity of the involved symbolic expressions. Similar behavior is therefore expected for even more complex model classes (ADM1-R1 or ADM1). In such cases, more advanced methods for assessing observability are required.

A practical application of model classes higher than the ADM1-R3 (e.g. ADM1-R2) is thus not anticipated for monitoring and control schemes due to the lack of online measurements of individual VFAs. It was therefore not further simplified into submodels and no further observability and identifiability analyses were pursued.

4 Conclusion

The models ADM1-R4 and ADM1-R3 were analyzed for observability and identifiability using differential algebraic and geometric approaches. With the former, observability of the ADM1-R4 was successfully shown. However, the algebraic approach failed for the full ADM1-R3 if only typical measurements at agricultural biogas plants were considered. In this scenario though, the geometric approach succeeded to show observability and identifiability for both ADM1-R3 and ADM1-R4, and exhibited a higher computational efficiency. This emphasizes that the ADM1 simplifications of Weinrich and Nelles [15] are indeed promising for state and parameter estimation as well as process automation for agricultural AD plants.

Acknowledgment

The authors are thankful for funding from German Federal Ministry of Food and Agriculture of the junior research group on simulation, monitoring and control of anaerobic digestion plants (grant 2219NR333). S. H. thanks Terrance Wilms for his encouragement and advice.

Appendix

The ADM1 simplifications of Weinrich and Nelles [15] have been transformed into standard control notation. This section summarizes the model equations and parameters of all successfully investigated models, starting with the simplest model structures. The following notation was applied:

- x_i - states (mass concentrations of the species involved),
- y_i - measurements
- u - control variable (feed volume flow)
- ξ_i - time-variant, uncertain parameters (inlet mass concentration)
- θ_i - time-variant parameters
- c_i - (aggregated) time-invariant parameters
- a_{ij} - time-invariant stoichiometric coefficients

States and inlet concentrations are usually given in g/l.³ The feed volume flow is stated in l/d. Units of states, inputs and measurements are summarized in Table 4. Units of all model parameters can be reviewed in [28].

Table 4: Units of states, inputs and measurements of all described models.

Symbol	Description	Unit
x_i	states	g/l
ξ_i	inlet concentrations	g/l
u	feed volume flow	l/d
\dot{V}_g	biogas volume flow	l/d
p_{ch4}	partial pressure of methane	bar
p_{co2}	partial pressure of carbon dioxide	bar
pH	pH value	—
S_{IN}	inorganic nitrogen concentration	g/l
TS	total solids content	—
VS	volatile solids content	—
S_{ac}	acetic acid concentration	g/l

ADM1-R4 Models

Aside from the ADM1-R4, the following models were analyzed: BMR4+B, BMR4+A, and BMR4.

ADM1-R4

State vector:

$$x = [S_{\text{ch4}}, S_{\text{IC}}, S_{\text{IN}}, S_{\text{h2o}}, X_{\text{ch}}, X_{\text{pr}}, X_{\text{li}}, X_{\text{bac}}, X_{\text{ash}}, S_{\text{ch4,gas}}, S_{\text{co2,gas}}]^T \quad (15)$$

Differential equations:

$$\dot{x}_1 = c_1 (\xi_1 - x_1) u + a_{11}\theta_1 x_5 + a_{12}\theta_2 x_6 + a_{13}\theta_3 x_7 - c_2 x_1 + c_3 x_{10} \quad (16a)$$

$$\dot{x}_2 = c_1 (\xi_2 - x_2) u + a_{21}\theta_1 x_5 + a_{22}\theta_2 x_6 + a_{23}\theta_3 x_7 - c_2 x_2 + c_4 x_{11} \quad (16b)$$

$$\dot{x}_3 = c_1 (\xi_3 - x_3) u - a_{31}\theta_1 x_5 + a_{32}\theta_2 x_6 - a_{33}\theta_3 x_7 \quad (16c)$$

$$\dot{x}_4 = c_1 (\xi_4 - x_4) u - a_{41}\theta_1 x_5 - a_{42}\theta_2 x_6 - a_{43}\theta_3 x_7 \quad (16d)$$

$$\dot{x}_5 = c_1 (\xi_5 - x_5) u - \theta_1 x_5 + a_{54}\theta_4 x_8 \quad (16e)$$

³For improved numerical stability, it is advised to express the water concentration S_{h2o} in kg/l. This levels out the large differences in numerical values present for a typically watery fermenter content (high values of S_{h2o} compared with all other species).

$$\dot{x}_6 = c_1 (\xi_6 - x_6) u - \theta_2 x_6 + a_{64} \theta_4 x_8 \quad (16f)$$

$$\dot{x}_7 = c_1 (\xi_7 - x_7) u - \theta_3 x_7 + a_{74} \theta_4 x_8 \quad (16g)$$

$$\dot{x}_8 = c_1 (\xi_8 - x_8) u + a_{81} \theta_1 x_5 + a_{82} \theta_2 x_6 + a_{83} \theta_3 x_7 - \theta_4 x_8 \quad (16h)$$

$$\dot{x}_9 = c_1 (\xi_9 - x_9) u \quad (16i)$$

$$\dot{x}_{10} = c_{15} x_{10}^3 + c_{16} x_{10}^2 x_{11} + c_{17} x_{10} x_{11}^2 + c_{18} x_{10}^2 + c_{19} x_{10} x_{11} + c_{20} x_{10} + c_5 x_1 \quad (16j)$$

$$\dot{x}_{11} = c_{17} x_{11}^3 + c_{16} x_{10} x_{11}^2 + c_{15} x_{10}^2 x_{11} + c_{19} x_{11}^2 + c_{18} x_{10} x_{11} + c_{21} x_{11} + c_5 x_2 \quad (16k)$$

a_{ij} are the absolute values of the entries of the petersen matrix given in Tab. 6. i denotes the column (component) and j the row (process). For brevity, only those entries with an absolute value $\neq 1$ or 0 were denoted specifically.

Measurements:

$$y_1 = \dot{V}_g = c_6 x_{10}^2 + c_7 x_{10} x_{11} + c_8 x_{11}^2 + c_9 x_{10} + c_{10} x_{11} + c_{11} \quad (17a)$$

$$y_2 = p_{\text{ch4}} = c_{12} x_{10} \quad (17b)$$

$$y_3 = p_{\text{co2}} = c_{13} x_{11} \quad (17c)$$

$$y_4 = S_{\text{IN}} = x_3 \quad (17d)$$

$$y_5 = TS = 1 - \frac{1}{c_{14}} x_4 \quad (17e)$$

$$y_6 = VS = 1 - \frac{1}{c_{14} - x_4} x_9 \quad (17f)$$

Tab. 5 summarizes the aggregated parameters c_i and the time-variant parameters θ_i used for ADM1-R4 and its submodels.

BMR4+B

The state vector remains as in (15). Differential equations:

$$\dot{x}_1 = c_1 (\xi_1 - x_1) u + a_{11} \theta_1 x_5 + a_{12} \theta_2 x_6 + a_{13} \theta_3 x_7 + a_{14} \theta_4 x_8 - c_2 x_1 + c_3 x_{10} \quad (18a)$$

$$\dot{x}_2 = c_1 (\xi_2 - x_2) u + a_{21} \theta_1 x_5 + a_{22} \theta_2 x_6 + a_{23} \theta_3 x_7 + a_{24} \theta_4 x_8 - c_2 x_2 + c_4 x_{11} \quad (18b)$$

$$\dot{x}_3 = c_1 (\xi_3 - x_3) u - a_{31} \theta_1 x_5 + a_{32} \theta_2 x_6 - a_{33} \theta_3 x_7 + a_{34} \theta_4 x_8 \quad (18c)$$

$$\dot{x}_4 = c_1 (\xi_4 - x_4) u - a_{41} \theta_1 x_5 - a_{42} \theta_2 x_6 - a_{43} \theta_3 x_7 - a_{44} \theta_4 x_8 \quad (18d)$$

$$\dot{x}_5 = c_1 (\xi_5 - x_5) u - \theta_1 x_5 \quad (18e)$$

$$\dot{x}_6 = c_1 (\xi_6 - x_6) u - \theta_2 x_6 \quad (18f)$$

$$\dot{x}_7 = c_1 (\xi_7 - x_7) u - \theta_3 x_7 \quad (18g)$$

$$\dot{x}_8 = c_1 (\xi_8 - x_8) u + a_{81} \theta_1 x_5 + a_{82} \theta_2 x_6 + a_{83} \theta_3 x_7 - a_{84} \theta_4 x_8 \quad (18h)$$

$$\dot{x}_9 = c_1 (\xi_9 - x_9) u \quad (18i)$$

$$\dot{x}_{10} = c_{15} x_{10}^3 + c_{16} x_{10}^2 x_{11} + c_{17} x_{10} x_{11}^2 + c_{18} x_{10}^2 + c_{19} x_{10} x_{11} + c_{20} x_{10} + c_5 x_1 \quad (18j)$$

$$\dot{x}_{11} = c_{17}x_{11}^3 + c_{16}x_{10}x_{11}^2 + c_{15}x_{10}^2x_{11} + c_{19}x_{11}^2 + c_{18}x_{10}x_{11} + c_{21}x_{11} + c_5x_2. \quad (18k)$$

Note that omitting model part A entails modified stoichiometric constants a_{ij} as given in Tab. 7. The other parameters remain the same and are summarized in Tab.5. The measurements remain as in (17).

BMR4+A

State vector:

$$x = [S_{\text{IN}}, S_{\text{H}_2\text{O}}, X_{\text{ch}}, X_{\text{pr}}, X_{\text{li}}, X_{\text{bac}}, X_{\text{ash}}, S_{\text{ch4,gas}}, S_{\text{co2,gas}}]^T \quad (19)$$

Differential equations, where a_{ij} are given in Tab. 6 and the remaining parameters in Tab.5:

$$\dot{x}_1 = c_1 (\xi_1 - x_1) u - a_{31}\theta_1x_3 + a_{32}\theta_2x_4 - a_{33}\theta_3x_5 \quad (20a)$$

$$\dot{x}_2 = c_1 (\xi_2 - x_2) u - a_{41}\theta_1x_3 - a_{42}\theta_2x_4 - a_{43}\theta_3x_5 \quad (20b)$$

$$\dot{x}_3 = c_1 (\xi_3 - x_3) u - \theta_1x_3 + a_{54}\theta_4x_6 \quad (20c)$$

$$\dot{x}_4 = c_1 (\xi_4 - x_4) u - \theta_2x_4 + a_{64}\theta_4x_6 \quad (20d)$$

$$\dot{x}_5 = c_1 (\xi_5 - x_5) u - \theta_3x_5 + a_{74}\theta_4x_6 \quad (20e)$$

$$\dot{x}_6 = c_1 (\xi_6 - x_6) u + a_{81}\theta_1x_3 + a_{82}\theta_2x_4 + a_{83}\theta_3x_5 - \theta_4x_6 \quad (20f)$$

$$\dot{x}_7 = c_1 (\xi_7 - x_7) u \quad (20g)$$

$$\begin{aligned} \dot{x}_8 = & c_{22}a_{11}\theta_1x_3 + c_{22}a_{12}\theta_2x_4 + c_{22}a_{13}\theta_3x_5 + c_{15}x_8^3 + c_{16}x_8^2x_9 + c_{17}x_8x_9^2 + c_{18}x_8^2 + \\ & + c_{19}x_8x_9 + c_{23}x_8 \end{aligned} \quad (20h)$$

$$\begin{aligned} \dot{x}_9 = & c_{22}a_{21}\theta_1x_3 + c_{22}a_{22}\theta_2x_4 + c_{22}a_{23}\theta_3x_5 + c_{17}x_9^3 + c_{16}x_8x_9^2 + c_{15}x_8^2x_9 + c_{19}x_9^2 + \\ & + c_{18}x_8x_9 + c_{23}x_9 \end{aligned} \quad (20i)$$

Measurements:

$$y_1 = \dot{V}_g = c_6x_8^2 + c_7x_8x_9 + c_8x_9^2 + c_9x_8 + c_{10}x_9 + c_{11}, \quad (21a)$$

$$y_2 = p_{\text{ch4}} = c_{12}x_8, \quad (21b)$$

$$y_3 = p_{\text{co2}} = c_{13}x_9, \quad (21c)$$

$$y_4 = S_{\text{IN}} = x_1, \quad (21d)$$

$$y_5 = TS = 1 - \frac{1}{c_{14}}x_2, \quad (21e)$$

$$y_6 = VS = 1 - \frac{1}{c_{14} - x_2}x_7. \quad (21f)$$

BMR4

The state vector remains as in (19). Differential equations:

$$\dot{x}_1 = c_1 (\xi_1 - x_1) u - a_{31}\theta_1 x_3 + a_{32}\theta_2 x_4 - a_{33}\theta_3 x_5 + a_{34}\theta_4 x_6 \quad (22a)$$

$$\dot{x}_2 = c_1 (\xi_2 - x_2) u - a_{41}\theta_1 x_3 - a_{42}\theta_2 x_4 - a_{43}\theta_3 x_5 - a_{44}\theta_4 x_6 \quad (22b)$$

$$\dot{x}_3 = c_1 (\xi_3 - x_3) u - \theta_1 x_3 \quad (22c)$$

$$\dot{x}_4 = c_1 (\xi_4 - x_4) u - \theta_2 x_4 \quad (22d)$$

$$\dot{x}_5 = c_1 (\xi_5 - x_5) u - \theta_3 x_5 \quad (22e)$$

$$\dot{x}_6 = c_1 (\xi_6 - x_6) u + a_{81}\theta_1 x_3 + a_{82}\theta_2 x_4 + a_{83}\theta_3 x_5 - a_{84}\theta_4 x_6 \quad (22f)$$

$$\dot{x}_7 = c_1 (\xi_7 - x_7) u \quad (22g)$$

$$\begin{aligned} \dot{x}_8 = & c_{22}a_{11}\theta_1 x_3 + c_{22}a_{12}\theta_2 x_4 + c_{22}a_{13}\theta_3 x_5 + c_{22}a_{14}\theta_4 x_6 + c_{15}x_8^3 + c_{16}x_8^2 x_9 + \\ & + c_{17}x_8 x_9^2 + c_{18}x_8^2 + c_{19}x_8 x_9 + c_{23}x_8 \end{aligned} \quad (22h)$$

$$\begin{aligned} \dot{x}_9 = & c_{22}a_{21}\theta_1 x_3 + c_{22}a_{22}\theta_2 x_4 + c_{22}a_{23}\theta_3 x_5 + c_{22}a_{24}\theta_4 x_6 + c_{17}x_9^3 + c_{16}x_8 x_9^2 + \\ & + c_{15}x_8^2 x_9 + c_{19}x_9^2 + c_{18}x_8 x_9 + c_{23}x_9 \end{aligned} \quad (22i)$$

a_{ij} are given in Tab. 7 and the remaining parameters in Tab.5. The measurements remain as in (21).

Table 5: Aggregated and time-variant parameters and notation of ADM1-R4 and its submodels.

Aggregated notation	Notation by Weinrich and Nelles [15]
u	\dot{V}_f
θ_1	k_{ch}
θ_2	k_{pr}
θ_3	k_{li}
θ_4	k_{dec}
c_1	V_l^{-1}
c_2	$k_L a$
c_3	$k_L a K_{H,\text{ch4}} \bar{R}T$
c_4	$k_L a K_{H,\text{co2}} \bar{R}T$
c_5	$k_L a V_l V_g^{-1}$
c_6	$k_p p_0^{-1} \left(\bar{R}T \bar{M}_{\text{ch4}}^{-1} \right)^2$
c_7	$2k_p p_0^{-1} \left(\bar{R}T \right)^2 \bar{M}_{\text{ch4}}^{-1} \bar{M}_{\text{co2}}^{-1}$
c_8	$k_p p_0^{-1} \left(\bar{R}T \bar{M}_{\text{co2}}^{-1} \right)^2$
c_9	$k_p p_0^{-1} \bar{R}T \bar{M}_{\text{ch4}}^{-1} (2p_{\text{h2o}} - p_0)$
c_{10}	$k_p p_0^{-1} \bar{R}T \bar{M}_{\text{co2}}^{-1} (2p_{\text{h2o}} - p_0)$
c_{11}	$k_p p_0^{-1} (p_{\text{h2o}} - p_0) p_{\text{h2o}}$
c_{12}	$\bar{R}T \bar{M}_{\text{ch4}}^{-1}$
c_{13}	$\bar{R}T \bar{M}_{\text{co2}}^{-1}$
c_{14}	ρ_l
c_{15}	$-k_p p_0^{-1} V_g^{-1} \left(\bar{R}T \bar{M}_{\text{ch4}}^{-1} \right)^2$
c_{16}	$-2k_p p_0^{-1} V_g^{-1} \left(\bar{R}T \right)^2 \bar{M}_{\text{ch4}}^{-1} \bar{M}_{\text{co2}}^{-1}$
c_{17}	$-k_p p_0^{-1} V_g^{-1} \left(\bar{R}T \bar{M}_{\text{co2}}^{-1} \right)^2$
c_{18}	$-k_p p_0^{-1} V_g^{-1} \bar{R}T \bar{M}_{\text{ch4}}^{-1} (2p_{\text{h2o}} - p_0)$
c_{19}	$-k_p p_0^{-1} V_g^{-1} \bar{R}T \bar{M}_{\text{co2}}^{-1} (2p_{\text{h2o}} - p_0)$
c_{20}	$-k_L a V_l V_g^{-1} K_{H,\text{ch4}} \bar{R}T - k_p p_0^{-1} V_g^{-1} (p_{\text{h2o}} - p_0) p_{\text{h2o}}$
c_{21}	$-k_L a V_l V_g^{-1} K_{H,\text{co2}} \bar{R}T - k_p p_0^{-1} V_g^{-1} (p_{\text{h2o}} - p_0) p_{\text{h2o}}$
c_{22}	$V_l V_g^{-1}$
c_{23}	$-k_p p_0^{-1} V_g^{-1} (p_{\text{h2o}} - p_0) p_{\text{h2o}}$

Table 6: Petersen matrix of ADM1-R4, derived from [28].

Component $i \rightarrow$	1	2	3	4	5	6	7	8	9	10	11	
j Process \downarrow	S_{ch4}	S_{IC}	S_{IN}	S_{h2o}	X_{ch}	X_{pr}	X_{li}	X_{bac}	X_{ash}	$S_{\text{ch4,gas}}$	$S_{\text{co2,gas}}$	Process rate r_j
1 Fermentation X_{ch}	0.2482	0.6809	-0.0207	-0.0456	-1			0.1372				$\theta_1 x_5$
2 Fermentation X_{pr}	0.3221	0.7954	0.1689	-0.4588		-1		0.1723				$\theta_2 x_6$
3 Fermentation X_{li}	0.6393	0.5817	-0.0344	-0.4152			-1	0.2286				$\theta_3 x_7$
4 Decay X_{bac}					0.18	0.77	0.05	-1				$\theta_4 x_8$
5 Phase transition S_{ch4}	-1									c_{22}		$c_2 x_1 - c_3 x_{10}$
6 Phase transition S_{IC}		-1									c_{22}	$c_2 x_2 - c_4 x_{11}$

Table 7: Petersen matrix of BMR4+B, derived from [28].

Component $i \rightarrow$	1	2	3	4	5	6	7	8	9	10	11	
j Process \downarrow	S_{ch4}	S_{IC}	S_{IN}	S_{h2o}	X_{ch}	X_{pr}	X_{li}	X_{bac}	X_{ash}	$S_{\text{ch4,gas}}$	$S_{\text{co2,gas}}$	Process rate r_j
1 Fermentation X_{ch}	0.2482	0.6809	-0.0207	-0.0456	-1			0.1372				$\theta_1 x_5$
2 Fermentation X_{pr}	0.3221	0.7954	0.1689	-0.4588		-1		0.1723				$\theta_2 x_6$
3 Fermentation X_{li}	0.6393	0.5817	-0.0344	-0.4152			-1	0.2286				$\theta_3 x_7$
4 Decay X_{bac}	0.3246	0.7641	0.1246	-0.3822				-0.8312				$\theta_4 x_8$
5 Phase transition S_{ch4}	-1									c_{22}		$c_2 x_1 - c_3 x_{10}$
6 Phase transition S_{IC}		-1									c_{22}	$c_2 x_2 - c_4 x_{11}$

ADM1-R3 Models

Aside from ADM1-R3, the following models were analyzed: BMR3+AC, BMR3+BC, and BMR3+ABC.

ADM1-R3

State vector:

$$x = [S_{ac}, S_{ch4}, S_{IC}, S_{IN}, S_{h2o}, X_{ch}, X_{pr}, X_{li}, X_{bac}, X_{ac}, X_{ash}, \dots, S_{ion}, S_{ac-}, S_{hco3-}, S_{nh3}, S_{ch4,gas}, S_{co2,gas}]^T \quad (23)$$

Differential equations:

$$\dot{x}_1 = c_1 (\xi_1 - x_1) u + a_{11}\theta_1 x_6 + a_{12}\theta_2 x_7 + a_{13}\theta_3 x_8 - a_{14}\theta_5 \frac{x_1 x_{10}}{\theta_6 + x_1} I_{ac} \quad (24a)$$

$$\dot{x}_2 = c_1 (\xi_2 - x_2) u + a_{21}\theta_1 x_6 + a_{22}\theta_2 x_7 + a_{23}\theta_3 x_8 - c_5 x_2 + c_6 x_{16} + a_{24}\theta_5 \frac{x_1 x_{10}}{\theta_6 + x_1} I_{ac} \quad (24b)$$

$$\dot{x}_3 = c_1 (\xi_3 - x_3) u + a_{31}\theta_1 x_6 + a_{32}\theta_2 x_7 - a_{33}\theta_3 x_8 - c_5 x_3 + c_5 x_{14} + c_7 x_{17} + a_{34}\theta_5 \frac{x_1 x_{10}}{\theta_6 + x_1} I_{ac} \quad (24c)$$

$$\dot{x}_4 = c_1 (\xi_4 - x_4) u - a_{41}\theta_1 x_6 + a_{42}\theta_2 x_7 - a_{43}\theta_3 x_8 - a_{44}\theta_5 \frac{x_1 x_{10}}{\theta_6 + x_1} I_{ac} \quad (24d)$$

$$\dot{x}_5 = c_1 (\xi_5 - x_5) u - a_{51}\theta_1 x_6 - a_{52}\theta_2 x_7 - a_{53}\theta_3 x_8 + a_{54}\theta_5 \frac{x_1 x_{10}}{\theta_6 + x_1} I_{ac} \quad (24e)$$

$$\dot{x}_6 = c_1 (\xi_6 - x_6) u - \theta_1 x_6 + a_{65}\theta_4 x_9 + a_{66}\theta_4 x_{10} \quad (24f)$$

$$\dot{x}_7 = c_1 (\xi_7 - x_7) u - \theta_2 x_7 + a_{75}\theta_4 x_9 + a_{76}\theta_4 x_{10} \quad (24g)$$

$$\dot{x}_8 = c_1 (\xi_8 - x_8) u - \theta_3 x_8 + a_{85}\theta_4 x_9 + a_{86}\theta_4 x_{10} \quad (24h)$$

$$\dot{x}_9 = c_1 (\xi_9 - x_9) u + a_{91}\theta_1 x_6 + a_{92}\theta_2 x_7 + a_{93}\theta_3 x_8 - \theta_4 x_9 \quad (24i)$$

$$\dot{x}_{10} = c_1 (\xi_{10} - x_{10}) u - \theta_4 x_{10} + \theta_5 \frac{x_1 x_{10}}{\theta_6 + x_1} I_{ac} \quad (24j)$$

$$\dot{x}_{11} = c_1 (\xi_{11} - x_{11}) u \quad (24k)$$

$$\dot{x}_{12} = c_1 (\xi_{12} - x_{12}) u \quad (24l)$$

$$\dot{x}_{13} = c_{29} (x_1 - x_{13}) - c_9 x_{13} S_{H+} \quad (24m)$$

$$\dot{x}_{14} = c_{30} (x_3 - x_{14}) - c_{10} x_{14} S_{H+} \quad (24n)$$

$$\dot{x}_{15} = c_{31} (x_4 - x_{15}) - c_{11} x_{15} S_{H+} \quad (24o)$$

$$\dot{x}_{16} = c_{22} x_{16}^3 + c_{23} x_{16}^2 x_{17} + c_{24} x_{16} x_{17}^2 + c_{25} x_{16}^2 + c_{26} x_{16} x_{17} + c_{12} x_2 + c_{27} x_{16} \quad (24p)$$

$$\dot{x}_{17} = c_{24} x_{17}^3 + c_{23} x_{16} x_{17}^2 + c_{22} x_{16}^2 x_{17} + c_{26} x_{17}^2 + c_{25} x_{16} x_{17} + c_{12} x_3 - c_{12} x_{14} + c_{28} x_{17} \quad (24q)$$

I_{ac} and S_{H+} are defined as

$$I_{ac} = \frac{c_3}{c_3 + S_{H+}^{c_2}} \frac{x_4}{x_4 + c_8} \frac{\theta_7}{\theta_7 + x_{15}} \quad (25)$$

$$S_{H+} = -\frac{\Phi}{2} + \frac{1}{2} \sqrt{\Phi^2 + c_4}, \text{ where} \quad (26)$$

$$\Phi = x_{12} + \frac{x_4 - x_{15}}{17} - \frac{x_{14}}{44} - \frac{x_{13}}{60}. \quad (27)$$

The absolute values of the stoichiometric coefficients a_{ij} are given in the petersen matrix of ADM1-R3, Tab. 9. Note that for all ADM1-R3 models, definition and indexing of parameters and stoichiometric constants is independent from all ADM1-R4 models.

Measurements:

$$y_1 = \dot{V}_g = c_{13}x_{16}^2 + c_{14}x_{16}x_{17} + c_{15}x_{17}^2 + c_{16}x_{16} + c_{17}x_{17} + c_{18} \quad (28a)$$

$$y_2 = p_{\text{ch4}} = c_{19}x_{16} \quad (28b)$$

$$y_3 = p_{\text{co2}} = c_{20}x_{17} \quad (28c)$$

$$y_4 = pH = -\log_{10} S_{\text{H}^+} \quad (28d)$$

$$y_5 = S_{\text{IN}} = x_4 \quad (28e)$$

$$y_6 = TS = 1 - \frac{1}{c_{21}}x_5, \quad (28f)$$

$$y_7 = VS = 1 - \frac{1}{c_{21} - x_5}x_{11} \quad (28g)$$

$$y_8 = S_{\text{ac}} = x_1 \quad (28h)$$

Tab. 8 summarizes the aggregated parameters c_i and the time-variant parameters θ_i used for ADM1-R3 and all of its submodels.

BMR3+ABC

State vector:

$$x = [S_{\text{ac}}, S_{\text{ch4}}, S_{\text{IC}}, S_{\text{IN}}, S_{\text{h2o}}, X_{\text{ch}}, X_{\text{pr}}, X_{\text{li}}, X_{\text{bac}}, X_{\text{ac}}, X_{\text{ash}}, S_{\text{ch4,gas}}, S_{\text{co2,gas}}]^T \quad (29)$$

Differential equations:

$$\dot{x}_1 = c_1 (\xi_1 - x_1) u + a_{11}\theta_1 x_6 + a_{12}\theta_2 x_7 + a_{13}\theta_3 x_8 - a_{14}\theta_5 \frac{x_1 x_{10}}{\theta_6 + x_1} \frac{x_4}{x_4 + c_8} \quad (30a)$$

$$\dot{x}_2 = c_1 (\xi_2 - x_2) u + a_{21}\theta_1 x_6 + a_{22}\theta_2 x_7 + a_{23}\theta_3 x_8 - c_5 x_2 + c_6 x_{12} + a_{24}\theta_5 \frac{x_1 x_{10}}{\theta_6 + x_1} \frac{x_4}{x_4 + c_8} \quad (30b)$$

$$\dot{x}_3 = c_1 (\xi_3 - x_3) u + a_{31}\theta_1 x_6 + a_{32}\theta_2 x_7 - a_{33}\theta_3 x_8 - c_5 x_3 + c_7 x_{13} + a_{34}\theta_5 \frac{x_1 x_{10}}{\theta_6 + x_1} \frac{x_4}{x_4 + c_8} \quad (30c)$$

$$\dot{x}_4 = c_1 (\xi_4 - x_4) u - a_{41}\theta_1 x_6 + a_{42}\theta_2 x_7 - a_{43}\theta_3 x_8 - a_{44}\theta_5 \frac{x_1 x_{10}}{\theta_6 + x_1} \frac{x_4}{x_4 + c_8} \quad (30d)$$

$$\dot{x}_5 = c_1 (\xi_5 - x_5) u - a_{51}\theta_1 x_6 - a_{52}\theta_2 x_7 - a_{53}\theta_3 x_8 + a_{54}\theta_5 \frac{x_1 x_{10}}{\theta_6 + x_1} \frac{x_4}{x_4 + c_8} \quad (30e)$$

$$\dot{x}_6 = c_1 (\xi_6 - x_6) u - \theta_1 x_6 + a_{65}\theta_4 x_9 + a_{66}\theta_4 x_{10} \quad (30f)$$

$$\dot{x}_7 = c_1 (\xi_7 - x_7) u - \theta_2 x_7 + a_{75}\theta_4 x_9 + a_{76}\theta_4 x_{10} \quad (30g)$$

$$\dot{x}_8 = c_1 (\xi_8 - x_8) u - \theta_3 x_8 + a_{85}\theta_4 x_9 + a_{86}\theta_4 x_{10} \quad (30h)$$

$$\dot{x}_9 = c_1 (\xi_9 - x_9) u + a_{91}\theta_1 x_6 + a_{92}\theta_2 x_7 + a_{93}\theta_3 x_8 - \theta_4 x_9 \quad (30i)$$

$$\dot{x}_{10} = c_1 (\xi_{10} - x_{10}) u - \theta_4 x_{10} + \theta_5 \frac{x_1 x_{10}}{\theta_6 + x_1} \frac{x_4}{x_4 + c_8} \quad (30j)$$

$$\dot{x}_{11} = c_1 (\xi_{11} - x_{11}) u \quad (30k)$$

$$\dot{x}_{12} = c_{22} x_{12}^3 + c_{23} x_{12}^2 x_{13} + c_{24} x_{12} x_{13}^2 + c_{25} x_{12}^2 + c_{26} x_{12} x_{13} + c_{12} x_2 + c_{27} x_{12} \quad (30l)$$

$$\dot{x}_{13} = c_{24} x_{13}^3 + c_{23} x_{12} x_{13}^2 + c_{22} x_{12}^2 x_{13} + c_{26} x_{13}^2 + c_{25} x_{12} x_{13} + c_{12} x_3 + c_{28} x_{13} \quad (30m)$$

a_{ij} should be taken from Tab. 9. The other involved parameters are given in Tab. 8.

Measurements:

$$y_1 = \dot{V}_g = c_{13} x_{12}^2 + c_{14} x_{12} x_{13} + c_{15} x_{13}^2 + c_{16} x_{12} + c_{17} x_{13} + c_{18} \quad (31a)$$

$$y_2 = p_{ch4} = c_{19} x_{12} \quad (31b)$$

$$y_3 = p_{co2} = c_{20} x_{13} \quad (31c)$$

$$y_4 = S_{IN} = x_4 \quad (31d)$$

$$y_5 = TS = 1 - \frac{1}{c_{21}} x_5 \quad (31e)$$

$$y_6 = VS = 1 - \frac{1}{c_{21} - x_5} x_{11} \quad (31f)$$

$$y_7 = S_{ac} = x_1 \quad (31g)$$

BMR3+BC

The state vector remains as in (29). Differential equations:

$$\begin{aligned} \dot{x}_1 = & c_1 (\xi_1 - x_1) u + a_{11} \theta_1 x_6 + a_{12} \theta_2 x_7 + a_{13} \theta_3 x_8 - a_{14} \theta_5 \frac{x_1 x_{10}}{\theta_6 + x_1} \frac{x_4}{x_4 + c_8} + a_{15} \theta_4 x_9 + \\ & + a_{16} \theta_4 x_{10} \end{aligned} \quad (32a)$$

$$\begin{aligned} \dot{x}_2 = & c_1 (\xi_2 - x_2) u + a_{21} \theta_1 x_6 + a_{22} \theta_2 x_7 + a_{23} \theta_3 x_8 - c_5 x_2 + c_6 x_{12} + a_{24} \theta_5 \frac{x_1 x_{10}}{\theta_6 + x_1} \frac{x_4}{x_4 + c_8} + \\ & + a_{25} \theta_4 x_9 + a_{26} \theta_4 x_{10} \end{aligned} \quad (32b)$$

$$\begin{aligned} \dot{x}_3 = & c_1 (\xi_3 - x_3) u + a_{31} \theta_1 x_6 + a_{32} \theta_2 x_7 - a_{33} \theta_3 x_8 - c_5 x_3 + c_7 x_{13} + a_{34} \theta_5 \frac{x_1 x_{10}}{\theta_6 + x_1} \frac{x_4}{x_4 + c_8} + \\ & + a_{35} \theta_4 x_9 + a_{36} \theta_4 x_{10} \end{aligned} \quad (32c)$$

$$\begin{aligned} \dot{x}_4 = & c_1 (\xi_4 - x_4) u - a_{41} \theta_1 x_6 + a_{42} \theta_2 x_7 - a_{43} \theta_3 x_8 - a_{44} \theta_5 \frac{x_1 x_{10}}{\theta_6 + x_1} \frac{x_4}{x_4 + c_8} + a_{45} \theta_4 x_9 + \\ & + a_{46} \theta_4 x_{10} \end{aligned} \quad (32d)$$

$$\begin{aligned} \dot{x}_5 = & c_1 (\xi_5 - x_5) u - a_{51} \theta_1 x_6 - a_{52} \theta_2 x_7 - a_{53} \theta_3 x_8 + a_{54} \theta_5 \frac{x_1 x_{10}}{\theta_6 + x_1} \frac{x_4}{x_4 + c_8} - a_{55} \theta_4 x_9 + \\ & - a_{56} \theta_4 x_{10} \end{aligned} \quad (32e)$$

$$\dot{x}_6 = c_1 (\xi_6 - x_6) u - \theta_1 x_6 \quad (32f)$$

$$\dot{x}_7 = c_1 (\xi_7 - x_7) u - \theta_2 x_7 \quad (32g)$$

$$\dot{x}_8 = c_1 (\xi_8 - x_8) u - \theta_3 x_8 \quad (32h)$$

$$\dot{x}_9 = c_1 (\xi_9 - x_9) u + a_{91} \theta_1 x_6 + a_{92} \theta_2 x_7 + a_{93} \theta_3 x_8 - a_{95} \theta_4 x_9 + a_{96} \theta_4 x_{10} \quad (32i)$$

$$\dot{x}_{10} = c_1 (\xi_{10} - x_{10}) u - \theta_4 x_{10} + \theta_5 \frac{x_1 x_{10}}{\theta_6 + x_1} \frac{x_4}{x_4 + c_8} \quad (32j)$$

$$\dot{x}_{11} = c_1 (\xi_{11} - x_{11}) u \quad (32k)$$

$$\dot{x}_{12} = c_{22}x_{12}^3 + c_{23}x_{12}^2x_{13} + c_{24}x_{12}x_{13}^2 + c_{25}x_{12}^2 + c_{26}x_{12}x_{13} + c_{12}x_2 + c_{27}x_{12} \quad (32l)$$

$$\dot{x}_{13} = c_{24}x_{13}^3 + c_{23}x_{12}x_{13}^2 + c_{22}x_{12}^2x_{13} + c_{26}x_{13}^2 + c_{25}x_{12}x_{13} + c_{12}x_3 + c_{28}x_{13} \quad (32m)$$

Note that omitting model part A entails modified stoichiometric constants a_{ij} as given in Tab. 10. The other involved parameters remain the same. They are given in Tab. 8.

Measurements:

$$y_1 = \dot{V}_g = c_{13}x_{12}^2 + c_{14}x_{12}x_{13} + c_{15}x_{13}^2 + c_{16}x_{12} + c_{17}x_{13} + c_{18} \quad (33a)$$

$$y_2 = p_{ch4} = c_{19}x_{12} \quad (33b)$$

$$y_3 = p_{co2} = c_{20}x_{13} \quad (33c)$$

$$y_4 = S_{IN} = x_4 \quad (33d)$$

$$y_5 = TS = 1 - \frac{1}{c_{21}}x_5 \quad (33e)$$

$$y_6 = VS = 1 - \frac{1}{c_{21} - x_5}x_{11} \quad (33f)$$

$$y_7 = S_{ac} = x_1 \quad (33g)$$

BMR3+AC

State vector:

$$x = [S_{ac}, S_{IN}, S_{h2o}, X_{ch}, X_{pr}, X_{li}, X_{bac}, X_{ac}, X_{ash}, S_{ch4,gas}, S_{co2,gas}]^T \quad (34)$$

Differential equations:

$$\dot{x}_1 = c_1 (\xi_1 - x_1) u + a_{11}\theta_1x_4 + a_{12}\theta_2x_5 + a_{13}\theta_3x_6 - a_{14}\theta_5 \frac{x_1 x_8}{\theta_6 + x_1} \frac{x_2}{x_2 + c_8} \quad (35a)$$

$$\dot{x}_2 = c_1 (\xi_2 - x_2) u - a_{41}\theta_1x_4 + a_{42}\theta_2x_5 - a_{43}\theta_3x_6 - a_{44}\theta_5 \frac{x_1 x_8}{\theta_6 + x_1} \frac{x_2}{x_2 + c_8} \quad (35b)$$

$$\dot{x}_3 = c_1 (\xi_3 - x_3) u - a_{51}\theta_1x_4 - a_{52}\theta_2x_5 - a_{53}\theta_3x_6 + a_{54}\theta_5 \frac{x_1 x_8}{\theta_6 + x_1} \frac{x_2}{x_2 + c_8} \quad (35c)$$

$$\dot{x}_4 = c_1 (\xi_4 - x_4) u - \theta_1x_4 + a_{65}\theta_4x_7 + a_{66}\theta_4x_8 \quad (35d)$$

$$\dot{x}_5 = c_1 (\xi_5 - x_5) u - \theta_2x_5 + a_{75}\theta_4x_7 + a_{76}\theta_4x_8 \quad (35e)$$

$$\dot{x}_6 = c_1 (\xi_6 - x_6) u - \theta_3x_6 + a_{85}\theta_4x_7 + a_{86}\theta_4x_8 \quad (35f)$$

$$\dot{x}_7 = c_1 (\xi_7 - x_7) u + a_{91}\theta_1x_4 + a_{92}\theta_2x_5 + a_{93}\theta_3x_6 - \theta_4x_7 \quad (35g)$$

$$\dot{x}_8 = c_1 (\xi_8 - x_8) u + \theta_5 \frac{x_1 x_8}{\theta_6 + x_1} \frac{x_2}{x_2 + c_8} - \theta_4x_8 \quad (35h)$$

$$\dot{x}_9 = c_1 (\xi_9 - x_9) u \quad (35i)$$

$$\begin{aligned} \dot{x}_{10} = & c_{32}a_{21}\theta_1x_4 + c_{32}a_{22}\theta_2x_5 + c_{32}a_{23}\theta_3x_6 + c_{32}a_{24}\theta_5 \frac{x_1 x_8}{\theta_6 + x_1} \frac{x_2}{x_2 + c_8} + \\ & c_{22}x_{10}^3 + c_{23}x_{10}^2x_{11} + c_{24}x_{10}x_{11}^2 + c_{25}x_{10}^2 + c_{26}x_{10}x_{11} + c_{33}x_{10} \end{aligned} \quad (35j)$$

$$\begin{aligned} \dot{x}_{11} = & c_{32}a_{31}\theta_1x_4 + c_{32}a_{32}\theta_2x_5 - c_{32}a_{33}\theta_3x_6 + c_{32}a_{34}\theta_5\frac{x_1x_8}{\theta_6+x_1}\frac{x_2}{x_2+c_8} + \\ & c_{24}x_{11}^3 + c_{23}x_{10}x_{11}^2 + c_{22}x_{10}^2x_{11} + c_{26}x_{11}^2 + c_{25}x_{10}x_{11} + c_{33}x_{11} \end{aligned} \quad (35k)$$

a_{ij} should be taken from Tab. 9. The involved parameters remain the same. They are given in Tab. 8. Measurements:

$$y_1 = \dot{V}_g = c_{13}x_{10}^2 + c_{14}x_{10}x_{11} + c_{15}x_{11}^2 + c_{16}x_{10} + c_{17}x_{11} + c_{18} \quad (36a)$$

$$y_2 = p_{ch4} = c_{19}x_{10} \quad (36b)$$

$$y_3 = p_{co2} = c_{20}x_{11} \quad (36c)$$

$$y_4 = S_{IN} = x_2 \quad (36d)$$

$$y_5 = TS = 1 - \frac{1}{c_{21}}x_3 \quad (36e)$$

$$y_6 = VS = 1 - \frac{1}{c_{21} - x_3}x_9 \quad (36f)$$

$$y_7 = S_{ac} = x_1 \quad (36g)$$

BMR3+A

The state vector remains as in (34). Differential equations:

$$\dot{x}_1 = c_1(\xi_1 - x_1)u + a_{11}\theta_1x_4 + a_{12}\theta_2x_5 + a_{13}\theta_3x_6 - a_{14}\theta_5\frac{x_1x_8}{\theta_6+x_1} \quad (37a)$$

$$\dot{x}_2 = c_1(\xi_2 - x_2)u - a_{41}\theta_1x_4 + a_{42}\theta_2x_5 - a_{43}\theta_3x_6 - a_{44}\theta_5\frac{x_1x_8}{\theta_6+x_1} \quad (37b)$$

$$\dot{x}_3 = c_1(\xi_3 - x_3)u - a_{51}\theta_1x_4 - a_{52}\theta_2x_5 - a_{53}\theta_3x_6 + a_{54}\theta_5\frac{x_1x_8}{\theta_6+x_1} \quad (37c)$$

$$\dot{x}_4 = c_1(\xi_4 - x_4)u - \theta_1x_4 + a_{65}\theta_4x_7 + a_{66}\theta_4x_8 \quad (37d)$$

$$\dot{x}_5 = c_1(\xi_5 - x_5)u - \theta_2x_5 + a_{75}\theta_4x_7 + a_{76}\theta_4x_8 \quad (37e)$$

$$\dot{x}_6 = c_1(\xi_6 - x_6)u - \theta_3x_6 + a_{85}\theta_4x_7 + a_{86}\theta_4x_8 \quad (37f)$$

$$\dot{x}_7 = c_1(\xi_7 - x_7)u + a_{91}\theta_1x_4 + a_{92}\theta_2x_5 + a_{93}\theta_3x_6 - \theta_4x_7 \quad (37g)$$

$$\dot{x}_8 = c_1(\xi_8 - x_8)u + \theta_5\frac{x_1x_8}{\theta_6+x_1} - \theta_4x_8 \quad (37h)$$

$$\dot{x}_9 = c_1(\xi_9 - x_9)u \quad (37i)$$

$$\begin{aligned} \dot{x}_{10} = & c_{32}a_{21}\theta_1x_4 + c_{32}a_{22}\theta_2x_5 + c_{32}a_{23}\theta_3x_6 + c_{32}a_{24}\theta_5\frac{x_1x_8}{\theta_6+x_1} + \\ & c_{22}x_{10}^3 + c_{23}x_{10}^2x_{11} + c_{24}x_{10}x_{11}^2 + c_{25}x_{10}^2 + c_{26}x_{10}x_{11} + c_{33}x_{10} \end{aligned} \quad (37j)$$

$$\begin{aligned} \dot{x}_{11} = & c_{32}a_{31}\theta_1x_4 + c_{32}a_{32}\theta_2x_5 - c_{32}a_{33}\theta_3x_6 + c_{32}a_{34}\theta_5\frac{x_1x_8}{\theta_6+x_1} + \\ & c_{24}x_{11}^3 + c_{23}x_{10}x_{11}^2 + c_{22}x_{10}^2x_{11} + c_{26}x_{11}^2 + c_{25}x_{10}x_{11} + c_{33}x_{11} \end{aligned} \quad (37k)$$

a_{ij} should be taken from Tab. 9. The involved parameters remain the same. They are given in Tab. 8. Measurements are computed according to (36).

BMR3

The state vector remains as in (34). Differential equations:

$$\begin{aligned} \dot{x}_1 = & c_1 (\xi_1 - x_1) u + a_{11}\theta_1 x_4 + a_{12}\theta_2 x_5 + a_{13}\theta_3 x_6 - a_{14}\theta_5 \frac{x_1 x_8}{\theta_6 + x_1} + a_{15}\theta_4 x_7 + \\ & + a_{16}\theta_4 x_8 \end{aligned} \quad (38a)$$

$$\begin{aligned} \dot{x}_2 = & c_1 (\xi_2 - x_2) u - a_{41}\theta_1 x_4 + a_{42}\theta_2 x_5 - a_{43}\theta_3 x_6 - a_{44}\theta_5 \frac{x_1 x_8}{\theta_6 + x_1} + a_{45}\theta_4 x_7 + \\ & + a_{46}\theta_4 x_8 \end{aligned} \quad (38b)$$

$$\begin{aligned} \dot{x}_3 = & c_1 (\xi_3 - x_3) u - a_{51}\theta_1 x_4 - a_{52}\theta_2 x_5 - a_{53}\theta_3 x_6 + a_{54}\theta_5 \frac{x_1 x_8}{\theta_6 + x_1} - a_{55}\theta_4 x_7 + \\ & - a_{56}\theta_4 x_8 \end{aligned} \quad (38c)$$

$$\dot{x}_4 = c_1 (\xi_4 - x_4) u - \theta_1 x_4 \quad (38d)$$

$$\dot{x}_5 = c_1 (\xi_5 - x_5) u - \theta_2 x_5 \quad (38e)$$

$$\dot{x}_6 = c_1 (\xi_6 - x_6) u - \theta_3 x_6 \quad (38f)$$

$$\dot{x}_7 = c_1 (\xi_7 - x_7) u + a_{91}\theta_1 x_4 + a_{92}\theta_2 x_5 + a_{93}\theta_3 x_6 - a_{95}\theta_4 x_7 + a_{96}\theta_4 x_8 \quad (38g)$$

$$\dot{x}_8 = c_1 (\xi_8 - x_8) u + \theta_5 \frac{x_1 x_8}{\theta_6 + x_1} - \theta_4 x_8 \quad (38h)$$

$$\dot{x}_9 = c_1 (\xi_9 - x_9) u \quad (38i)$$

$$\begin{aligned} \dot{x}_{10} = & c_{32}a_{21}\theta_1 x_4 + c_{32}a_{22}\theta_2 x_5 + c_{32}a_{23}\theta_3 x_6 + c_{32}a_{24}\theta_5 \frac{x_1 x_8}{\theta_6 + x_1} + c_{32}a_{25}\theta_4 x_7 + \\ & + c_{32}a_{26}\theta_4 x_8 + c_{22}x_{10}^3 + c_{23}x_{10}^2 x_{11} + c_{24}x_{10}x_{11}^2 + c_{25}x_{10}^2 + c_{26}x_{10}x_{11} + c_{33}x_{10} \end{aligned} \quad (38j)$$

$$\begin{aligned} \dot{x}_{11} = & c_{32}a_{31}\theta_1 x_4 + c_{32}a_{32}\theta_2 x_5 - c_{32}a_{33}\theta_3 x_6 + c_{32}a_{34}\theta_5 \frac{x_1 x_8}{\theta_6 + x_1} + c_{32}a_{35}\theta_4 x_7 + \\ & + c_{32}a_{36}\theta_4 x_8 + c_{24}x_{11}^3 + c_{23}x_{10}x_{11}^2 + c_{22}x_{10}^2 x_{11} + c_{26}x_{11}^2 + c_{25}x_{10}x_{11} + c_{33}x_{11} \end{aligned} \quad (38k)$$

a_{ij} should be taken from Tab. 10. The involved parameters remain the same. They are given in Tab. 8. Measurements are computed according to (36).

Table 8: Aggregated and time-variant parameters and notation of ADM1-R3 and its submodels.

Aggregated notation	Notation by Weinrich and Nelles [15]
u	\dot{V}_f
θ_1	k_{ch}
θ_2	k_{pr}
θ_3	k_{li}
θ_4	k_{dec}
θ_5	$\mu_{m,\text{ac}}$
θ_6	$K_{S,\text{ac}}$
θ_7	$K_{I,\text{nh3}}$
c_1	V_l^{-1}
c_2	n_{ac}
c_3	$10^{-\frac{3}{2} \frac{pH_{UL,\text{ac}} + pH_{LL,\text{ac}}}{pH_{UL,\text{ac}} - pH_{LL,\text{ac}}}}$
c_4	$4K_W$
c_5	$k_L a$
c_6	$k_L a K_{H,\text{ch4}} \bar{R}T$
c_7	$k_L a K_{H,\text{co2}} \bar{R}T$
c_8	$K_{S,\text{IN}}$
c_9	$k_{AB,\text{ac}}$
c_{10}	$k_{AB,\text{co2}}$
c_{11}	$k_{AB,\text{IN}}$
c_{12}	$k_L a V_l V_g^{-1}$
c_{13}	$k_p p_0^{-1} (\bar{R}T \bar{M}_{\text{ch4}}^{-1})^2$
c_{14}	$2k_p p_0^{-1} (\bar{R}T)^2 \bar{M}_{\text{ch4}}^{-1} \bar{M}_{\text{co2}}^{-1}$
c_{15}	$k_p p_0^{-1} (\bar{R}T \bar{M}_{\text{co2}}^{-1})^2$
c_{16}	$k_p p_0^{-1} \bar{R}T \bar{M}_{\text{ch4}}^{-1} (2p_{\text{h2o}} - p_0)$
c_{17}	$k_p p_0^{-1} \bar{R}T \bar{M}_{\text{co2}}^{-1} (2p_{\text{h2o}} - p_0)$
c_{18}	$k_p p_0^{-1} (p_{\text{h2o}} - p_0) p_{\text{h2o}}$
c_{19}	$\bar{R}T \bar{M}_{\text{ch4}}^{-1}$
c_{20}	$\bar{R}T \bar{M}_{\text{co2}}^{-1}$
c_{21}	ρ_l
c_{22}	$-k_p V_g^{-1} p_0^{-1} (\bar{R}T \bar{M}_{\text{ch4}}^{-1})^2$
c_{23}	$-2k_p V_g^{-1} p_0^{-1} (\bar{R}T)^2 \bar{M}_{\text{ch4}}^{-1} \bar{M}_{\text{co2}}^{-1}$
c_{24}	$-k_p V_g^{-1} p_0^{-1} (\bar{R}T \bar{M}_{\text{co2}}^{-1})^2$
c_{25}	$-k_p V_g^{-1} p_0^{-1} \bar{R}T \bar{M}_{\text{ch4}}^{-1} (2p_{\text{h2o}} - p_0)$
c_{26}	$-k_p V_g^{-1} p_0^{-1} \bar{R}T \bar{M}_{\text{co2}}^{-1} (2p_{\text{h2o}} - p_0)$
c_{27}	$-k_L a V_l V_g^{-1} K_{H,\text{ch4}} \bar{R}T - k_p V_g^{-1} p_0^{-1} (p_{\text{h2o}} - p_0) p_{\text{h2o}}$
c_{28}	$-k_L a V_l V_g^{-1} K_{H,\text{co2}} \bar{R}T - k_p V_g^{-1} p_0^{-1} (p_{\text{h2o}} - p_0) p_{\text{h2o}}$
c_{29}	$k_{AB,\text{ac}} K_{a,\text{ac}}$
c_{30}	$k_{AB,\text{co2}} K_{a,\text{co2}}$
c_{31}	$k_{AB,\text{IN}} K_{a,\text{IN}}$
c_{32}	$V_l V_g^{-1}$
c_{33}	$-k_p V_g^{-1} p_0^{-1} (p_{\text{h2o}} - p_0) p_{\text{h2o}}$

Table 9: Petersen matrix of ADM1-R3, derived from [28].

Component $\mathbf{i} \rightarrow$	1	2	3	4	5	6	7	8	9	10	
\mathbf{j} Process \downarrow	S_{ac}	S_{ch4}	S_{IC}	S_{IN}	S_{h2o}	X_{ch}	X_{pr}	X_{li}	X_{bac}	X_{ac}	Process rate r_j
1 Fermentation X_{ch}	0.6555	0.0818	0.2245	-0.0169	-0.0574	-1			0.1125		$\theta_1 x_6$
2 Fermentation X_{pr}	0.9947	0.0696	0.1029	0.1746	-0.4767		-1		0.1349		$\theta_2 x_7$
3 Fermentation X_{li}	1.7651	0.1913	-0.6472	-0.0244	-0.4470			-1	0.1621		$\theta_3 x_8$
4 Methanogenesis S_{ac}	-26.5447	6.7367	18.4808	-0.1506	0.4778					1	$\theta_5 \frac{x_1}{\theta_6 + x_1} x_{10} I_{\text{ac}}$
5 Decay X_{bac}						0.18	0.77	0.05	-1		$\theta_4 x_9$
6 Decay X_{ac}						0.18	0.77	0.05		-1	$\theta_4 x_{10}$
	2	3	...	11	12	13	14	15	16	17	
	S_{ch4}	S_{IC}		X_{ash}	S_{ion}	$S_{\text{ac-}}$	$S_{\text{hco3-}}$	S_{nh3}	$S_{\text{ch4,gas}}$	$S_{\text{co2,gas}}$	
7 Dissoziation S_{ac}						-1					$c_{29} (x_{13} - x_1) + c_9 x_{13} S_{\text{H+}}$
8 Dissoziation S_{IC}							-1				$c_{30} (x_{14} - x_3) + c_{10} x_{14} S_{\text{H+}}$
9 Dissoziation S_{IN}								-1			$c_{31} (x_{15} - x_4) + c_{11} x_{15} S_{\text{H+}}$
10 Phase transition S_{ch4}	-1								c_{32}		$c_5 x_2 - c_6 x_{16}$
11 Phase transition S_{co2}		-1								c_{32}	$c_5 (x_3 - x_{14}) - c_7 x_{17}$

Table 10: Petersen matrix of BMR3+BC, derived from [28].

Component $\mathbf{i} \rightarrow$	1	2	3	4	5	6	7	8	9	10	11	12	13	
\mathbf{j} Process \downarrow	S_{ac}	S_{ch4}	S_{IC}	S_{IN}	S_{h2o}	X_{ch}	X_{pr}	X_{li}	X_{bac}	X_{ac}	X_{ash}	$S_{\text{ch4,gas}}$	$S_{\text{co2,gas}}$	Process rate r_j
1 Fermentation X_{ch}	0.6555	0.0818	0.2245	-0.0169	-0.0574	-1			0.1125					$\theta_1 x_6$
2 Fermentation X_{pr}	0.9947	0.0696	0.1029	0.1746	-0.4767		-1		0.1349					$\theta_2 x_7$
3 Fermentation X_{li}	1.7651	0.1913	-0.6472	-0.0244	-0.4470			-1	0.1621					$\theta_3 x_8$
4 Methanogenesis S_{ac}	-26.5447	6.7367	18.4808	-0.1506	0.4778					1				$\theta_5 \frac{x_1}{\theta_6 + x_1} x_{10} \frac{x_4}{x_4 + c_8}$
5 Decay X_{bac}	0.9722	0.0779	0.0873	0.1301	-0.3997				-0.8678					$\theta_4 x_9$
6 Decay X_{ac}	0.9722	0.0779	0.0873	0.1301	-0.3997				0.1322	-1				$\theta_4 x_{10}$
7 Phase transition S_{ch4}		-1										c_{32}		$c_5 x_2 - c_6 x_{12}$
8 Phase transition S_{co2}			-1										c_{32}	$c_5 x_3 - c_7 x_{13}$

Derivations for neglecting individual model parts

This section details the basic ideas behind neglecting individual model parts for both ADM1-R3 and ADM1-R4.

Neglecting model part A - stoichiometric degradation of microbial biomass to macro nutrients

Stoichiometric pathways of the ADM1 models can easily be derived from the rows of the petersen matrix, Tab. 9. In the original ADM1-R3/ADM1-R4, biomass (represented by the states X_{bac} and X_{ac}) is formed during degradation of macro nutrients (carbohydrates, proteins and lipids). Biomass in turn is decomposed into macro nutrients (decay of bacteria). This feedback can be removed by modifying the stoichiometry of biomass. Biomass is thereby not decomposed into macro nutrients, but into the stoichiometric degradation products of the macro nutrients directly. This delivers a modified stoichiometry, affecting the differential equations of S_{ac} , S_{ch4} , S_{IC} , S_{IN} , S_{h2o} , X_{ch} , X_{pr} , X_{li} , X_{bac} , and X_{ac} (depending on the used model class).

Neglecting model part B - gas solubility of CH_4 and CO_2

If CH_4 and CO_2 are assumed to be insoluble in the liquid phase, their stoichiometric formation therein (see e.g. (24b) and (24c)) has to be allocated to the gas phase. Gas transfer from liquid to gas phase is originally modeled by means of Henry's law. The according terms can be cut out, as well as the convection terms. Instead, the terms describing stoichiometric formation of CH_4 and CO_2 are normalized with the ratio of liquid and gas volume (V_l/V_g) and appear in the differential equations of $S_{\text{ch4,gas}}$ and $S_{\text{co2,gas}}$, respectively. This can be seen in e.g. (35j) and (35k). Computation of the gas volume flow remains as in the case with model part B.

Neglecting model part C - inhibition through nitrogen limitation

The second factor in the inhibition function I_{ac} describes inhibition through nitrogen limitation, see (25). Neglecting model part C is achieved by removing this factor, which reduces nonlinearities in the model. However, this does not allow to omit any of the state variables.

Neglecting model part D - inhibition through pH and ammonia

The full inhibition function I_{ac} is a major source of nonlinearity in the ADM1-R3. Neglecting model part D (inhibition through pH and ammonia) allows to cut out the first and last factor of I_{ac} , see (25). Consequently, S_{nh3} can be omitted in the state vector.

Neglecting model part E - computation of pH

Measuring the pH allows to infer S_{H+} directly because these two variables are linked via the negative common logarithm, (28d). Measuring the pH hence allows to interpret the variable S_{H+} as a time-variant parameter (without any associated differential equation). The states S_{ion} , S_{ac-} and S_{hco3-} (x_{12} to x_{14} in (23) and (24)) only appear in the computation of the charge balance Φ , (27) which is required to calculate S_{H+} . However, as S_{H+} can be directly determined from pH measurements, the states S_{ion} , S_{ac-} and S_{hco3-} become redundant. Their respective differential equations can be cut out of the system of equations. The resulting model BMR3+ABCD (not shown here) only incorporates dissociation between ammonium and ammonia. Yet, full inhibition through all three factors of I_{ac} (pH, nitrogen limitation and ammonia) are considered.

References

- [1] Ye Chen, Jay J. Cheng, and Kurt S. Creamer. Inhibition of anaerobic digestion process: A review. *Bioresource technology*, 99(10):4044–4064, 2008.
- [2] Daniel Gaida, Christian Wolf, and Michael Bongards. Feed control of anaerobic digestion processes for renewable energy production: A review. *Renewable and Sustainable Energy Reviews*, 68:869–875, 2017.
- [3] R. A. Flores-Estrella, V. Alcaraz-González, J. P. García-Sandoval, and V. González-Álvarez. Robust output disturbance rejection control for anaerobic digestion processes. *Journal of Process Control*, 75:15–23, 2019.
- [4] Víctor Alcaraz-González, Fabián Azael Fregoso-Sánchez, Víctor González-Alvarez, and Jean-Philippe Steyer. Multivariable robust regulation of alkalinities in continuous anaerobic digestion processes: Experimental validation. *Processes*, 9(7):1153, 2021.
- [5] Gerardo Lara-Cisneros, Ricardo Aguilar-López, Denis Dochain, and Ricardo Femat. On-line estimation of vfa concentration in anaerobic digestion via methane outflow rate measurements. *Computers & Chemical Engineering*, 94(4):250–256, 2016.
- [6] E. Rocha-Cozatl, M. Sbarciog, L. Dewasme, J. A. Moreno, and A. Vande Wouwer. State and input estimation of an anaerobic digestion reactor using a continuous-discrete unknown input observer. *IFAC-PapersOnLine*, 48(8):129–134, 2015.
- [7] Eric Mauky, Sören Weinrich, Hans-Joachim Nägele, H. Fabian Jacobi, Jan Liebetrau, and Michael Nelles. Model predictive control for demand-driven biogas production in full scale. *Chemical Engineering & Technology*, 39(4):652–664, 2016.
- [8] L. Dewasme, M. Sbarciog, E. Rocha-Cózatl, F. Haugen, and A. Vande Wouwer. State and unknown input estimation of an anaerobic digestion reactor with experimental validation. *Control Engineering Practice*, 85(4):280–289, 2019.
- [9] Pezhman Kazemi, Jean-Philippe Steyer, Christophe Bengoa, Josep Font, and Jaume Giralt. Robust data-driven soft sensors for online monitoring of volatile fatty acids in anaerobic digestion processes. *Processes*, 8(1):67, 2020.
- [10] Julie Jimenez, Eric Latrille, Jérôme Harmand, Angel Robles, José Ferrer, and Jean-Philippe Steyer. Instrumentation and control of anaerobic digestion processes: A review and some research challenges. *Reviews in Environmental Science and Bio/Technology*, 14(4):615–648, 2015.

- [11] O. Bernard, Z. Hadj-Sadok, D. Dochain, A. Genovesi, and J. P. Steyer. Dynamical model development and parameter identification for an anaerobic wastewater treatment process. *Biotechnology and bioengineering*, 75(4):424–438, 2001.
- [12] Shadi Attar and Finn Aakre Haugen. Comparison of different state estimator algorithms applied to a simulated anaerobic digestion reactor. In *Proceedings of The 59th Conference on Simulation and Modelling (SIMS 59)*, Linköping Electronic Conference Proceedings, pages 118–125. Linköping University Electronic Press, 2018.
- [13] D. J. Batstone, J. Keller, I. Angelidaki, S. V. Kalyuzhnyi, S. G. Pavlostathis, A. Rozzi, W.T.M. Sanders, H. Siegrist, and V. A. Vavilin. The IWA Anaerobic Digestion Model No 1 (ADM1). *Water science and technology: a journal of the International Association on Water Pollution Research*, 45(10):65–73, 2002.
- [14] Andres Donoso-Bravo, Johan Mailier, Cristina Martin, Jorge Rodríguez, César Arturo Aceves-Lara, and Alain Vande Wouwer. Model selection, identification and validation in anaerobic digestion: A review. *Water Research*, 45(17):5347–5364, 2011.
- [15] Sören Weinrich and Michael Nelles. Systematic simplification of the anaerobic digestion model no. 1 (ADM1) - model development and stoichiometric analysis: Application. *Bioresource technology*, 333:125124, 2021.
- [16] Sören Weinrich, Eric Mauky, Thomas Schmidt, Christian Krebs, Jan Liebetrau, and Michael Nelles. Systematic simplification of the anaerobic digestion model no. 1 (ADM1) - laboratory experiments and model application. *Bioresource technology*, 333:125104, 2021.
- [17] Milena Anguelova. *Observability and identifiability of nonlinear systems with applications in biology: Univ., Diss., 2007*. Doktorsavhandlingar vid Chalmers Tekniska Högskola. Chalmers Univ. of Technology, Göteborg, 2007.
- [18] Alejandro F. Villaverde, Antonio Barreiro, and Antonis Papachristodoulou. Structural identifiability of dynamic systems biology models. *PLoS computational biology*, 12(10):e1005153, 2016.
- [19] K. Maes, M. N. Chatzis, and G. Lombaert. Observability of nonlinear systems with unmeasured inputs. *Mechanical Systems and Signal Processing*, 130:378–394, 2019.
- [20] Oana-Teodora Chis, Julio R. Banga, and Eva Balsa-Canto. Structural identifiability of systems biology models: A critical comparison of methods. *PloS one*, 6(11):e27755, 2011.
- [21] Christian Wolf, Daniel Gaida, and Michael Bongards. Online-measurement systems for agricultural and industrial ad plants – a review and practice test. *Kompandium der Forschungsgemeinschaft :metabolon*, 2014.

- [22] K. Boe and I. Angelidaki. Pilot-scale application of an online vfa sensor for monitoring and control of a manure digester. *Water science and technology : a journal of the International Association on Water Pollution Research*, 66(11):2496–2503, 2012.
- [23] Jan Liebetrau and Diana Pfeiffer, editors. *Collection of Measurement Methods for Biogas*, volume 07 of *Biomass energy use*. Leipzig, Germany, 2 edition, 2020.
- [24] Dan Simon. *Optimal state estimation: Kalman, H-infinity, and nonlinear approaches*. Wiley-Interscience, Hoboken, NJ, 2006.
- [25] Sandra Díaz-Seoane, Xabier Rey-Barreiro, and Alejandro F. Villaverde. Strike-goldd 4.0: user-friendly, efficient analysis of structural identifiability and observability. *arxiv preprint*, arXiv:2207.07346, 2022.
- [26] Éric Walter and Luc Pronzato. *Identification of parametric models from experimental data*. Communications and control engineering series. Springer, London, 1997.
- [27] Nerea Martínez and Alejandro F. Villaverde. Nonlinear observability algorithms with known and unknown inputs: Analysis and implementation. *Mathematics*, 8(11):1876, 2020.
- [28] Sören Weinrich. *Praxisnahe Modellierung von Biogasanlagen: Systematische Vereinfachung des Anaerobic Digestion Model No. 1 (ADM1)*. PhD thesis, Universität Rostock, 2017.